IIETA International Information and Engineering Technology Association
Advancing the World of Information and Engineering

Revue d'Intelligence Artificielle
Vol. 36, No. 6, December, 2022, pp. 873-880
Journal homepage: http://iieta.org/journals/ria

A Case Study on Green Areas Change-Detection in Baghdad Using Artificial Intelligence

Rasha A. Ali[1*], Inaam A. Al-Bazzaz[2]

[1] Department of Architectural Engineering, College of Engineering, Al-Nahrain University, Jadriya, Baghdad 10070, Iraq
[2] Department of Architectural Engineering, College of Engineering, University of Baghdad, Jadriya, Baghdad 10070, Iraq

Corresponding Author Email: rasha.abdulkareem@nahrainuniv.edu.iq

https://doi.org/10.18280/ria.360607

Received: 1 November 2022
Accepted: 17 December 2022

Keywords:
artificial intelligence, change-detection, green areas, Baghdad, Machin learning, Adhamiya, urban fabric, CNN

ABSTRACT

As our cities expand and more people migrate into already crowded regions, green areas in cities minimize the effects of pollution and help reduce the urban heat island effect. Adhamiya in Baghdad is one of these urban fabrics that are suffering nowadays from crowded urban fabric with a shortage of green lungs; therefore, in response to these rapid changes and the need to keep an eye on them. This research presented a study based on artificial intelligence, which took advantage of HSV spectrum by restricting it to a group of colors that represent the colors of the green areas, as well as the generation of masks and use of them in the design of the study, as these technologies might provide speedy findings and contribute to the formulation of real-time judgments to examine examples of tissue changes and their influencing elements. Changes in the Green areas of urban fabric were analyzed using artificial intelligence has made considerable progress in exploring and deducing real-time changes and monitoring the environment. The results revealed a drop in the ratio of green areas from 22.45% to 5.46%. This serious indicator necessitates intervention by decision leaders to rectify the situation due to an important correlation between the decline in green areas and the increase in temperature in the region.

1. INTRODUCTION

Experts predict that the size of urban areas will rise by around three times between the years 2000 and 2030 [1]. It is well documented that the "structures of our cities" have a major impact on the occurrence of severe or extreme weather in the surrounding regional environment [2]. In rapidly expanding cities, especially in developing nations, these urban morphologies are characterized by impermeable surfaces, rapid loss of green area, and habitat fragmentation [3]. Green areas in cities, known collectively as urban forests, help lessen regional and local storm-related flooding and water pollution [4], improve air and water quality, moderate temperature, and promote nutrient cycling in soil, all while sequestering carbon [5]. So, Massive land transformations in urban areas—from green to concrete – result in an ever-increasing number of impermeable surfaces, resulting in an unnatural environment [6]. The green area (or leaf area) is frequently used to measure the ratio of green content in urban areas [7]. laying a scientific basis for optimizing green areas. The rates at which green spaces are planned within the spatial space of the urban environment depend on the local conditions of each city, and each of its residents is allocated a specific area of green areas; these rates vary from one country to another. For example, the percentage of green areas in German cities is 37%, in England it is 26% [8], and the American National Organization for Recreation and Parks considers that 25% is a minimum for modern cities [9], while 17.5% of land in Iraqi cities has been allocated for green spaces that have begun to shrink as a result of urban sprawl to fill them [10]. AI techniques are now becoming increasingly essential in categorization challenges [11]. Given the significance of the green cover within cities, the researcher examined this topic by comparing the green area in 2008 to the existing green area in 2022 [12].

To determine the green area, artificial intelligence techniques were employed to convert the green area from the satellite imagery [13]. Machine learning is insignificantly exploited for environmental needs. So should focus on AI to fight negative environmental impact as a major step to fight climate change [14]. The process involves converting the image's color format from RGB to HSV in order to exploit the image's color properties. This process extracts the image's green area features, as HSV is a cylinder color model that converts the RGB primary colors into aspects that are more intuitive to humans [15]. These contain hue, saturation, and value, similar to the Munsell Color System. After that the range of selected color shaped into a mask, the green area percentages are calculated and the necessary analyses are conducted. The accuracy of the study's calculations for the green area and the percentages for each year reached 92%, which is very remarkable.

Adhamiya is one of the oldest areas of Baghdad. The Adhamiya region first appeared during the Abbasid dynasty. The city was named after the Imam who was buried there, Abu Hanifa al-Numan. It is situated on the east bank of the Tigris River, about to the north of Baghdad. Figure 1 shows the impact on the Adhamiya area of just the loss of green areas and the replacement of gardens with homes.

2. RELATED WORKS

This section summarizes existing strategies for detecting changes in green areas using remotely sensed data:

- Khan et al. [16] construct a multi-resolution profile of the target area and create a collection of candidates bounding box recommendations that analyses satellite remote sensing imagery data to assess changes in green cover between 1987 and 2015. For current patches, the approach achieves an average classification rate of 91.6%. In addition, to demonstrate the scalability of the proposed forest change detection system, they subjectively evaluate the detected changes in the unlabeled image portions.

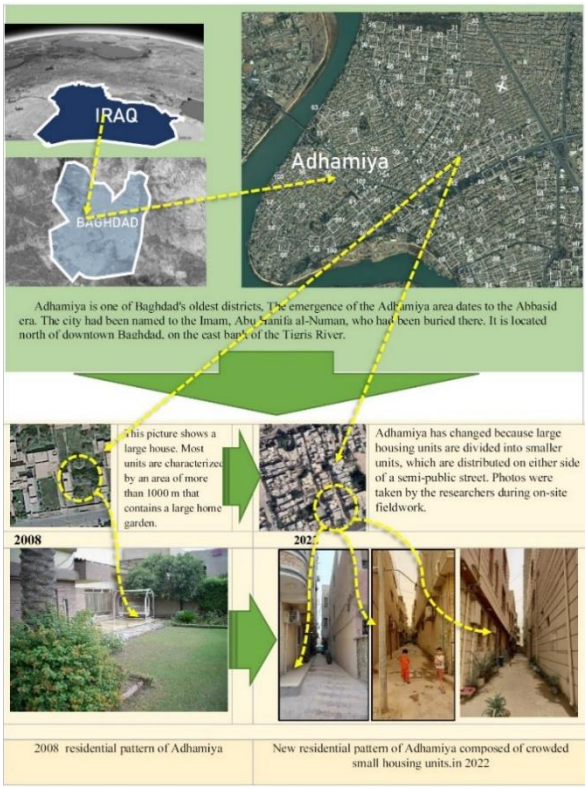

Figure 1. Field survey of the case study area, Adhamiya, performed by the authors [17]

- de Jong et al. [18] provide a convolutional neural network (CNN) for semantic segmentation is constructed in order to extract compressed picture characteristics and categorize observed changes between two temporally distinct photographs of the same scene. Thus, the suggested technique for change detection is unsupervised and may be implemented with any CNN model pre-trained for semantic segmentation [19].
- More et al. [20] employed spatiotemporal data from satellite pictures and a support vector machine (SVM) for classification to assess the effectiveness of GPU-based green area identification and monitoring from 2005 to 2019, they provide a framework for change detection and analysis in green areas, the method shows that, over a 15-year period, 50% of the entire green area was destroyed.
- Zhou et al. [21] utilize five deep learning models for change detection, including STANets (BASE, BAM, and PAM), SNUNet (Siam-NestedUNet), and BiT (Bitemporal image Transformer) using GF-2 satellite imagery; a high change detection label was developed. In the Core Region of Jiangbei New Area in Nanjing, China, between 2015 and 2021.
- Lechner et al. [22] provide a Breiman's random forest classifier and forest enterprise data, seven deciduous tree species and five coniferous tree species in the Austrian Biosphere Reserve Wienerwald (105,000 ha) were put into different groups. Sentinel-1 alone, including phenological markers and other variables generated from time series, could not provide adequate classification accuracy overall 55.7%.
- Fazelpoor et al. [23] discovered a spatiotemporal modifications and human influence of the border between Iran and Azerbaijan from 1984 to 2020. Using a supervised classification and geomorphological indicators, according to the findings, the active channel has contracted significantly 88.9 % with a lowering ratio of 16.6 m/year.

3. MATERIALS AND METHODS

This section explains the dataset utilized as well as the method used to construct the framework. The dataset used in the paper was created with the Adhamiya neighborhood Satellite images. The process is summarized by converting the images from RGB to HSV, then mask generation, and finally calculating the percentage of the green areas.

3.1 Dataset

The dataset utilized in this study was developed by the researcher particularly for this purpose; it consists of 208 high-resolution satellite images of the Adhamiya neighborhood in Baghdad. For accurate change detection, machine learning techniques such as Convolutional Neural Network (CNN) can be utilized to relieve the difficulty [24].

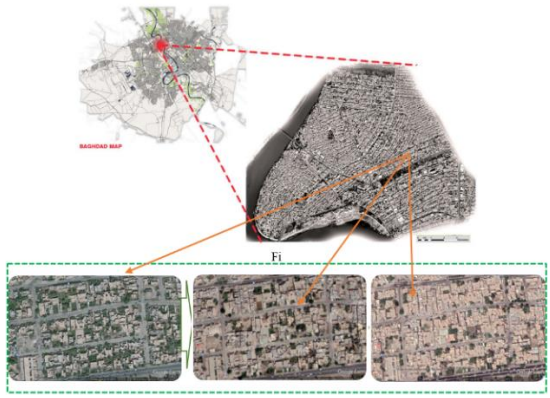

Figure 2. Baghdad-Adhamiya area map history. Shows a decline in green space between 2008 and 2022

Table 1. Dataset images specifications

Parameter	2008	2022
Source	Geoeye satellite image	Google satellite image
Resolution	60	30
Cloud cover	0%	0%
Size in pixels	2000 × 2000	2000 × 2000

It comprises of 104 images of various parts of the region taken in 2008, and the same number of images were taken in the same locations in 2022. Figure 2 depicts a map of Baghdad-Adhamiya area map history. Shows a decline in green space between 2008 and 2022, highlighting the selected portions as datasets. Table 1 show the images specifications used in dataset.

3.2 Methodology

This method relies heavily on the inventory of the color

spectrum, and it is vital to follow these stages to achieve effective results. Figure 3 depicts the method's steps:

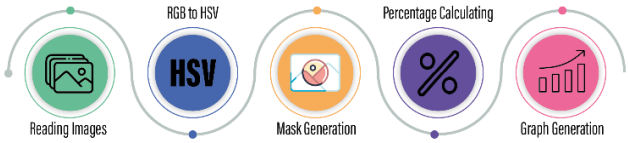

Figure 3. Methodology workflow

(1) Reading all of the images is the initial stage of the approach.

(2) Convert RGB image to HSV image:

i. Hue specifies the color's angle on the RGB color circle. A hue of 0 degrees is red, 120 degrees is green, and 240 degrees is blue.

ii. Saturation determines how much color is utilized. A color with a saturation of 100 percent is the clearest color conceivable, while a saturation of 0 percent produces grayscale.

iii. Value regulates the color's luminance. A color with zero percent brightness is pure black, while a color with one hundred percent brightness contains no black. The HSV color model is also referred to as HSB, including in P5.js, because this dimension is frequently referred to as brightness.

The conversion is done from RGB to HSV, because as we learned that HSV has to deal with gradients separately, and it is the best way to get a gradient to deal with it, in order to study the gradients, we need to make the threshold. Figure 4 shows the RGB to HSV example. This ensures that you get the best possible result. HSV ranges for the year (2022) is:

$$(H \rightarrow 70\text{-}105,\ S \rightarrow 25\text{-}255,\ V \rightarrow 25\text{-}255)$$

and for (2008) is:

$$(H \rightarrow 33\text{-}75,\ S \rightarrow 25\text{-}255,\ V \rightarrow 25\text{-}255)$$

(3) Mask Generation: The second stage of the image analysis procedure started when the range of the green areas' tonalities was identified after studying them for both years. This range was then turned into a mask. The input and source image are the converted image and the inputs are two values, with the lowest value representing the lowest gradient and the greatest value representing the widest color spectrum. In the Figure 5, it clear that the mask is made of two colors: black and white. The white parts of the mask represent the green parts, while the black parts represent the rest of the ingredients.

(4) Percentage Calculating: After making a mask, it turns out that the white is the green area. To find the percentage of green areas in each image, we divide the number of white points in the mask by the total number of pixels. It is easier to find similarities and differences between the two years. The percentage of green area Figure 6 is calculated by the equation:

$$Green\ Percentage = White\ area\ /\ Size\ of\ image \quad (1)$$

where:

- White area represents the green areas;
- Size of image is 2000 * 2000 px.

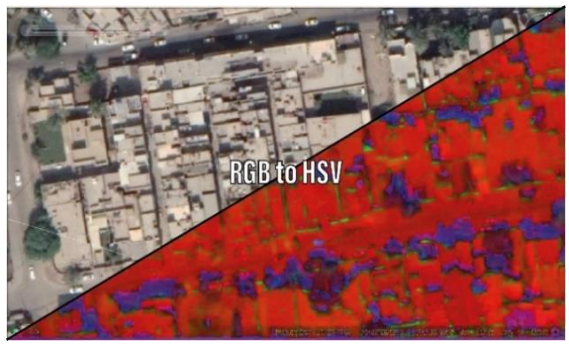

(a)

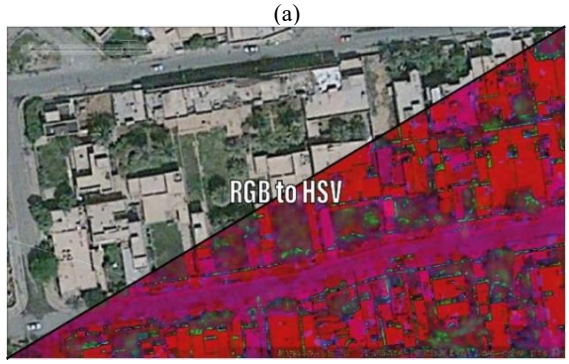

(b)

Figure 4. RGB to HSV example (a) 2022 (b) 2008

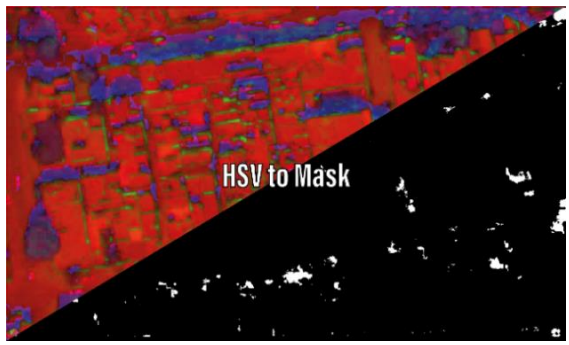

(a)

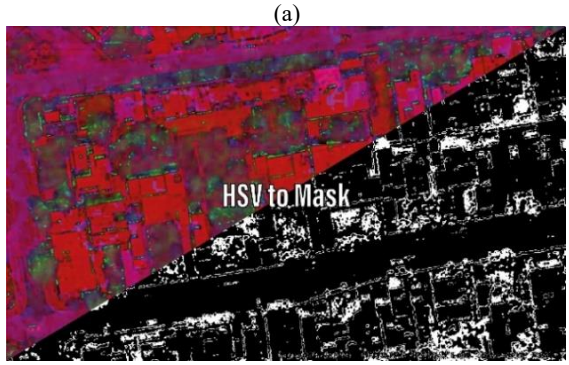

(b)

Figure 5. Mask generation example (a) 2022 (b) 2008

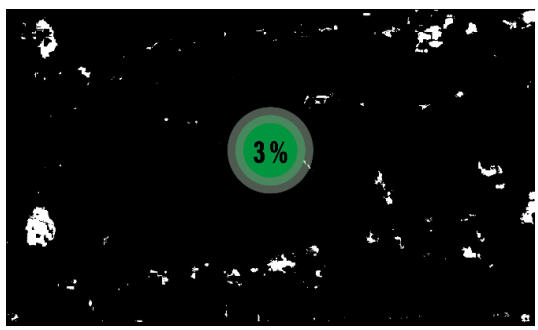

(a)

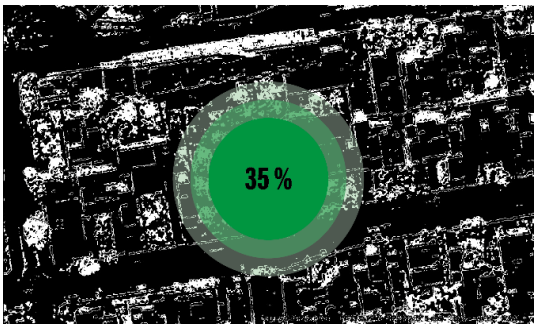

(b)

Figure 6. Green area percentage (a) 2022 (b) 2008

4. RESULTS

After completing the preceding stages and analysing the established dataset, the following results were obtained, which are displayed in the tables and graphs below:

Mask Generation Results: At this stage, a satisfactory result of 90% was reached, according to the Table 2 which displays the results obtained at the stage of mask generation, and based on the apparent results, it can be concluded that the method used in the research was largely successful in generating the correct mask for the green areas, with a record time of only 50 seconds for the entire dataset, and this time is Relatively suitable, because other methods that include training take a long time, but the results were very satisfactory.

Table 2. Mask generation results (sample of dataset)

2008 Image	2008 Mask	2022 Image	2022 Mask
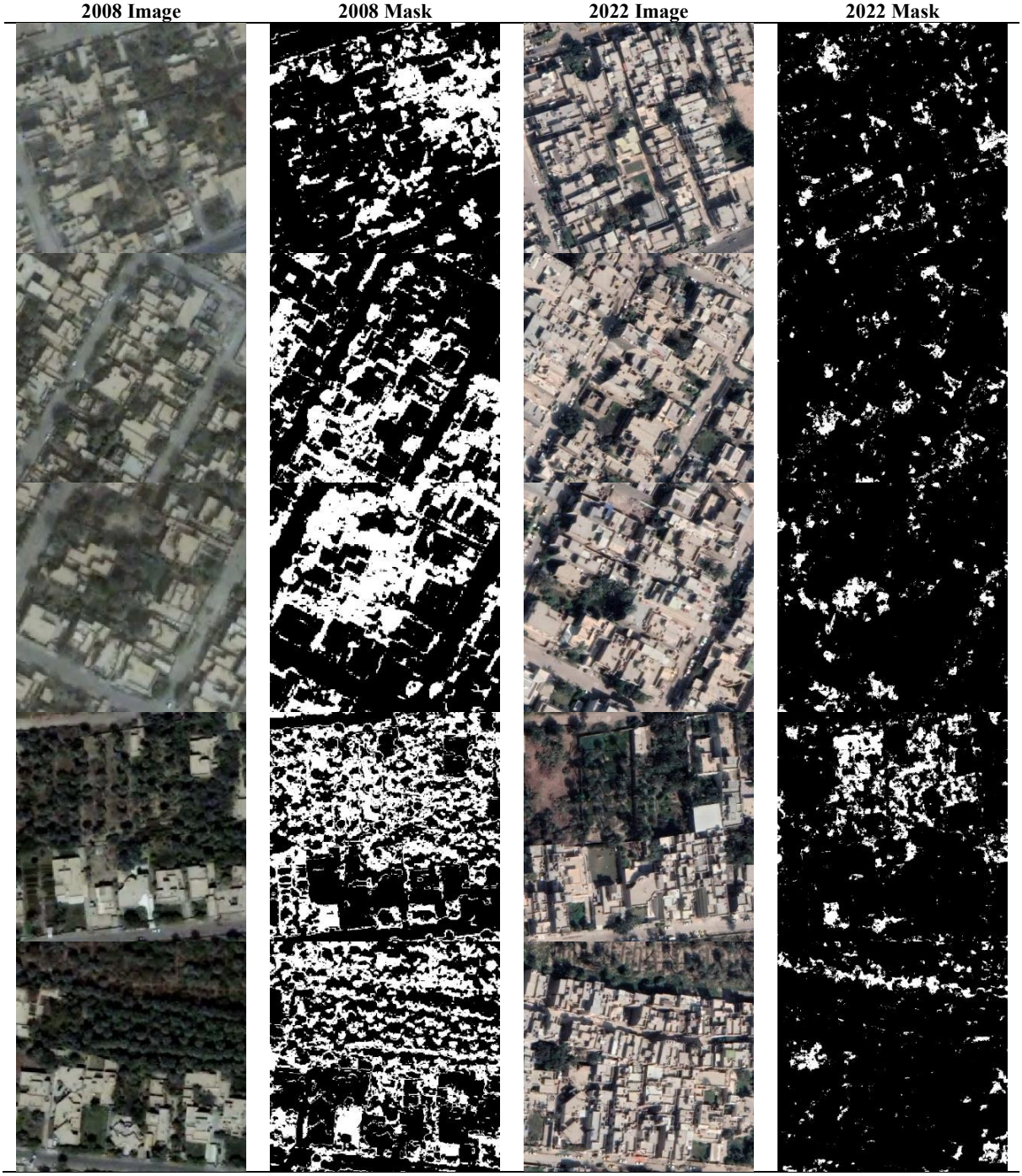			

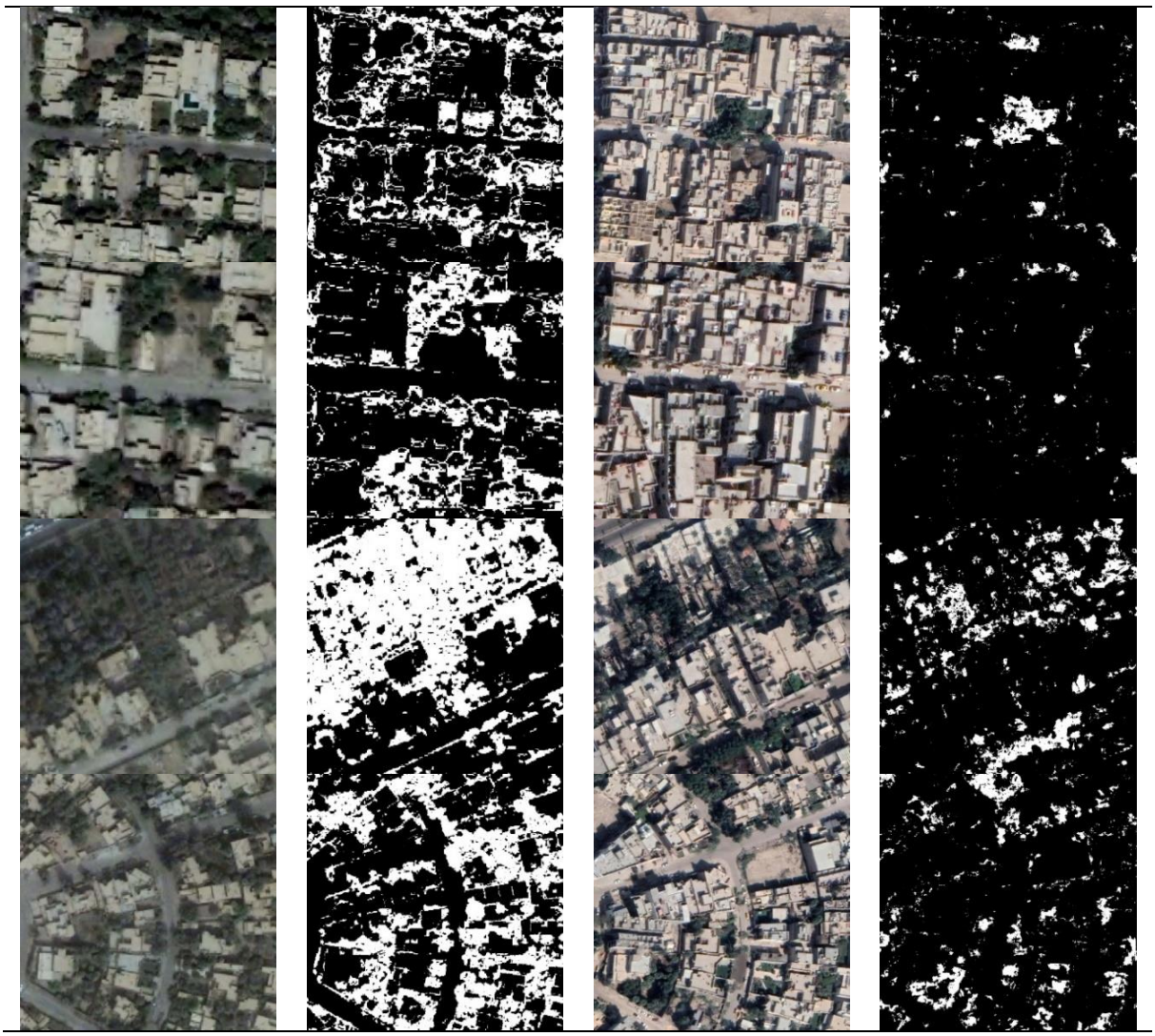

Green Area Percentage Results: Following the generation of the masks, the percentage of the green area is calculated, yielding the following results showed in Table 3.

Table 3. Green area percentage results

#	2008	2022	Status
1	24.22%	7.81%	↓
2	13.21%	6.33%	↓
3	23.95%	8.10%	↓
4	11.38%	6.73%	↓
5	16.99%	5.93%	↓
6	12.70%	5.71%	↓
7	15.31%	7.04%	↓
8	25.70%	6.82%	↓
9	22.51%	7.67%	↓
10	26.24%	8.22%	↓
11	27.26%	9.40%	↓
12	22.45%	6.88%	↓
13	27.66%	8.00%	↓
14	25.77%	5.65%	↓
15	27.62%	5.57%	↓
16	30.80%	6.10%	↓
17	20.20%	4.68%	↓
18	22.17%	5.11%	↓
19	22.38%	4.57%	↓
20	19.17%	4.94%	↓
21	34.88%	6.44%	↓
22	25.51%	2.78%	↓
23	27.27%	4.53%	↓
24	36.39%	4.27%	↓
25	30.62%	4.57%	↓
26	26.10%	2.46%	↓
27	25.50%	3.45%	↓
28	20.99%	4.31%	↓
29	20.29%	4.35%	↓
30	8.61%	3.02%	↓
31	25.34%	7.15%	↓
32	25.26%	9.74%	↓
33	12.09%	3.35%	↓
34	39.07%	14.06%	↓
35	35.57%	6.57%	↓
36	24.08%	4.55%	↓
37	23.75%	2.54%	↓
38	12.39%	1.23%	↓
39	18.85%	7.24%	↓
40	9.42%	1.80%	↓
41	20.99%	6.32%	↓
42	28.69%	4.23%	↓
43	25.24%	3.82%	↓
44	22.17%	2.66%	↓
45	26.29%	4.93%	↓
46	23.32%	2.45%	↓
47	23.04%	3.18%	↓
48	35.60%	4.64%	↓
49	21.10%	2.61%	↓
50	22.80%	2.38%	↓
51	14.85%	3.34%	↓
52	22.32%	2.18%	↓
53	20.33%	2.57%	↓
54	12.38%	1.45%	↓
55	14.03%	2.46%	↓

56	19.81%	1.60%	↓
57	28.62%	3.80%	↓
58	28.19%	3.77%	↓
59	31.69%	3.36%	↓
60	29.10%	5.06%	↓
61	30.36%	3.05%	↓
62	10.74%	1.61%	↓
63	16.22%	6.43%	↓
64	31.14%	16.19%	↓
65	50.85%	13.60%	↓
66	53.87%	10.26%	↓
67	15.13%	6.72%	↓
68	14.94%	7.75%	↓
69	28.04%	6.57%	↓
70	26.70%	6.28%	↓
71	14.18%	4.44%	↓
72	13.73%	5.31%	↓
73	8.85%	4.48%	↓
74	10.54%	4.52%	↓
75	3.30%	3.38%	↑
76	15.97%	5.58%	↓
77	15.09%	6.24%	↓
78	16.19%	7.46%	↓
79	28.01%	10.61%	↓
80	37.26%	10.35%	↓
81	16.10%	3.05%	↓
82	7.03%	5.06%	↓
83	1.12%	2.52%	↑
84	14.23%	3.76%	↓
85	15.37%	4.27%	↓
86	13.20%	4.82%	↓
87	7.09%	2.52%	↓
88	31.80%	11.61%	↓
89	21.95%	6.13%	↓
90	13.30%	4.98%	↓
91	26.29%	6.34%	↓
92	41.93%	7.91%	↓
93	24.62%	7.56%	↓
94	24.60%	9.88%	↓
95	14.58%	5.73%	↓
96	21.64%	4.46%	↓
97	41.59%	10.66%	↓
98	22.24%	4.22%	↓
99	25.46%	2.75%	↓
100	24.51%	4.78%	↓
101	20.94%	3.26%	↓
102	27.92%	4.38%	↓
103	25.41%	2.59%	↓
104	21.17%	7.61%	↓
Avg	**22.46%**	**5.46%**	↓

The results indicated that the average percentage of green areas in 2008 was 22.46%, while in 2022 it decreased to 5.46%, a 17% fall that is an alarming warning of a large decline in green areas. Table 3 shows that the amount of green area has dropped by a huge amount, and a high slope shows that large areas of green area have been lost.

The results based on confusion matrix:

Table 4. Confusion matrix for 2008 results

		Actual Values	
		Positives	**Negatives**
Predicated Values	**Positives**	48	6
	Negatives	4	47

Accuracy	90.48%
Precision	88.89%
Recall	92.31%
F1 Score	90.57%

Table 5. Confusion matrix for 2022 results

		Actual Values	
		Positives	**Negatives**
Predicated Values	**Positives**	51	3
	Negatives	5	45

Accuracy	92.31%
Precision	94.44%
Recall	91.07%
F1 Score	92.73%

On the basis of the data shown in Tables 4-5, it is clear that the acquired results are excellent, when comparing. Change in green areas percentages from 2008 to 2022 were taken from the system and are displayed in Table 1 to 5. Figures S1, S2 in the Supplementary Materials represent the spatial distribution for green areas results on map. When the system begins to record a decrease rate of change throughout the years 2008–2022, it becomes apparent that a significant shift has occurred.

5. CONCLUSIONS

The following conclusions were reached as a result of the preceding information and experiments:

(1) The method employed in this study greatly reduced the time required to generate masks.

(2) The method assisted in determining the proportion of green areas and comparing them between the two years, so enabling numerous studies to be conducted on this basis.

(3) By analysing numerous temperature scales, it was shown that the percentage of green regions is inversely proportional to the temperature, since locations with green areas have a greater temperature than those with few or no green areas Figure 7 and 8.

(4) The superiority of the results is due to the fact that the image in 2022 was obtained with newer and more advanced equipment; consequently, the resolution is better and the detecting technique is more exact and efficient.

(5) The housing problem played a significant role in Baghdad's loss of green spaces, particularly in the Adhamiya region, extensive buildings with large gardens vanished in the lack of a serious plan to address the situation, as a result of the housing crisis and rising real estate costs, houses were divided and their gardens were converted into small houses without trees.

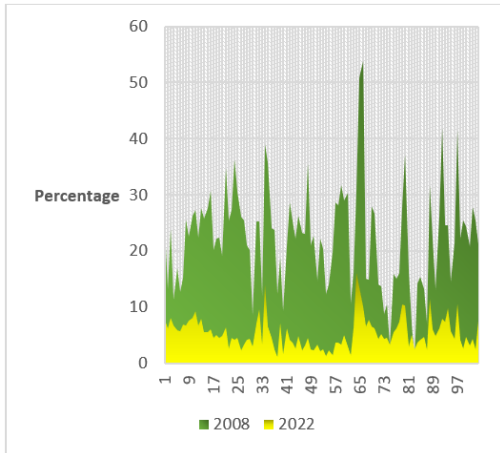

Figure 7. Green area percentage chart

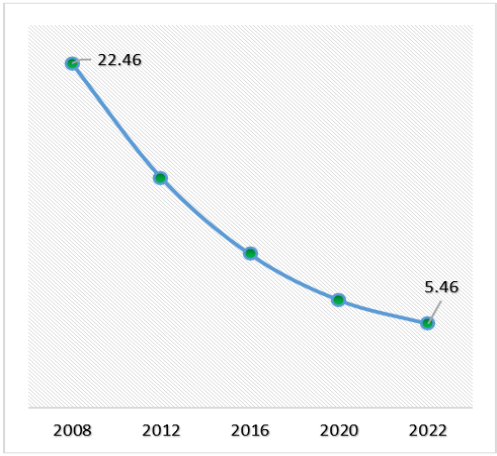

Figure 8. Green area average percentage change

Baghdad has seen a significant increase of green spaces since the 1930s, beginning with public gardens and parks and progressing through squares and planting walkways and open spaces overlapping between residential districts. And increasing the aesthetic value of the city, until this growth began to veer in the opposite direction since the ninth decade of the twentieth century, when the delay began in completing the implementation of development projects plans for the development of the city, particularly with regard to green spaces, while the period that followed the year 2008 was characterized by stagnation in the expansion of green spaces due to what The country witnessed turbulent conditions, weak oversimplification. All of this encouraged citizen to encroach on green spaces and change their use at random for purposes in an attempt to solve the problem of increasing population growth, rapid and uncontrolled urban expansion, which damaged the city's green spaces and lost an important aesthetic element, and caused an imbalance in the local environment's balance that it maintained. For decades, it has had a deleterious impact on the local climate.

As a result, it is necessary to pay attention to the expansion of green spaces within the city and work to remove and control the slums that occupy them, employing advanced artificial intelligence techniques that reduce the effort and time required for urban monitoring of the city while enabling adherence to the planned basic design.

REFERENCES

[1] McDonald, R.I., Mansur, A.V., Ascensão, F., et al. (2020). Research gaps in knowledge of the impact of urban growth on biodiversity. Nature Sustainability, 3(1): 16-24. https://doi.org/10.1038/s41893-019-0436-6

[2] Collier, C.G. (2006). The impact of urban areas on weather. Quarterly Journal of the Royal Meteorological Society: A Journal of the Atmospheric Sciences, Applied Meteorology and Physical Oceanography, 132(614): 1-25. https://doi.org/10.1256/qj.05.199

[3] Haaland, C., van Den Bosch, C.K. (2015). Challenges and strategies for urban green-space planning in cities undergoing densification: A review. Urban Forestry & Urban Greening, 14(4): 760-771. https://doi.org/10.1016/j.ufug.2015.07.009

[4] Cartier, K.M.S. (2021). Growing Equity in City Green Space. Available: https://eos.org/features/growing-equity-in-city-green-space.

[5] Elbasiouny, H., El-Ramady, H., Elbehiry, F., Rajput, V.D., Minkina, T., Mandzhieva, S. (2022). Plant nutrition under climate change and soil carbon sequestration. Sustainability, 14(2): 914. https://doi.org/10.3390/su14020914

[6] Milly, P.C.D., Wetherald, R.T., Dunne, K.A., Delworth, T.L. (2002). Increasing risk of great floods in a changing climate. Nature, 415(6871): 514-517. https://doi.org/10.1038/415514a

[7] Jia, H.R. Zhang, Y.C. (2022). Optimization of Street Tree Species Based on Green Plot Ratio. J. Urban Dev. Manag., 1(1): pp. 26-38. https://doi.org/10.56578/judm010104

[8] Paynter, P. (2011). Planning sustainable cities, global report on human settlements 2009. Australian Planner, 48(3): 243-244. https://doi.org/10.1080/07293682.2011.552434

[9] Allen, L.R., Barcelona, R.J. (2011). Recreation as a Developmental Experience: Theory Practice Research: New Directions for Youth Development, Number 130. John Wiley & Sons.

[10] http://wiki.dorar-aliraq.net/iraqilaws/law/5144.html.

[11] Veesam, V.S., Ravichandran, S., Babu, G.R.M. (2022). Deep neural networks for automatic facial expression recognition. Revue d'Intelligence Artificielle, 36(5): 809-814. https://doi.org/10.18280/ria.360520

[12] Hasan, A.M., Kadhim, A.A. (2020). Design and implementation of smart meter for smart city. Iraqi Journal of Information and Communication Technology, 3(3): 33-42. https://doi.org/10.31987/ijict.3.3.127

[13] Lu, C., Chen, M., Tian, G. (2022). Spatial-temporal evolution and influencing factors of urban green innovation efficiency in China. Journal of Environmental and Public Health, 2022: e4047572. https://doi.org/10.1155/2022/4047572

[14] Mah, P.M. Skalna, I., Pełech-Pilichowski, T., Muzam, J.M Munyeshuri, E., Uwakmfon, P.O., Mudoh, P. (2022). Integration of sensors and predictive analysis with machine learning as a modern tool for economic activities and a major step to fight against climate change. Journal of Green Economy and Low-Carbon Development, 1(1): 16-33. https://doi.org/10.56578/jgelcd010103

[15] Saini, P. (2021). Difference Between RGB, CMYK, HSV, and YIQ Color Models. Available: https://www.geeksforgeeks.org/difference-between-rgb-cmyk-hsv-and-yiq-color-models.

[16] Khan, S.H., He, X., Porikli, F., Bennamoun, M. (2017). Forest change detection in incomplete satellite images with deep neural networks. IEEE Transactions on Geoscience and Remote Sensing, 55(9): 5407-5423. https://doi.org/10.1109/TGrs.2017.2707528

[17] Ali, R.A. (2022). Advanced technology in genetic architecture, the role of artificial intelligence in genetic changes detecting and predicting in the -Adhamiya urban fabric. PHD Thesis, NON-Published, University of Baghdad, College of Engineering, Department of Architecture, 2022.

[18] de Jong, K.L., Bosman, A.S. (2019). Unsupervised change detection in satellite images using convolutional neural networks. In 2019 International Joint Conference on Neural Networks (IJCNN), pp. 1-8. https://doi.org/10.1109/IJCNN.2019.8851762

[19] Saha, S. (2018). A Comprehensive Guide to Convolutional Neural Networks—the ELI5 way. Available: https://towardsdatascience.com/a-comprehensive-guide-to-convolutional-neural-networks-the-eli5-way-3bd2b1164a53.
[20] More, N., Nikam, V.B., Banerjee, B. (2020). Machine learning on high performance computing for urban greenspace change detection: satellite image data fusion approach. International Journal of Image and Data Fusion, 11(3): 218-232. https://doi.org/10.1080/19479832.2020.1749142
[21] Zhou, S., Dong, Z., Wang, G. (2022). Machine-Learning-Based Change Detection of Newly Constructed Areas from GF-2 Imagery in Nanjing, China. Remote Sensing, 14(12): 2874. https://doi.org/10.3390/rs14122874
[22] Lechner, M., Dostálová, A., Hollaus, M., Atzberger, C., Immitzer, M. (2022). Combination of sentinel-1 and sentinel-2 data for tree species classification in a central European biosphere reserve. Remote Sensing, 14(11): 2687. https://doi.org/10.3390/rs14112687
[23] Fazelpoor, K., Martínez-Fernández, V., Yousefi, S., de Jalón, D.G. (2022). Remote sensing and machine learning techniques to monitor fluvial corridor evolution: The Aras River between Iran and Azerbaijan. In Computers in Earth and Environmental Sciences, pp. 289-297. https://doi.org/10.1016/B978-0-323-89861-4.00021-X
[24] Ayyıldız, H., Kalaycı, M. Tuncer, S.A. Çınar, A. Tuncer, T. (2022). Automated COVID-19 detection from WBC-DIFF scattergram images with hybrid CNN model using feature selection. Traitement du Signal, 39(2): 449-458. https://doi.org/10.18280/ts.390206

APPENDIX

Supplementary Materials

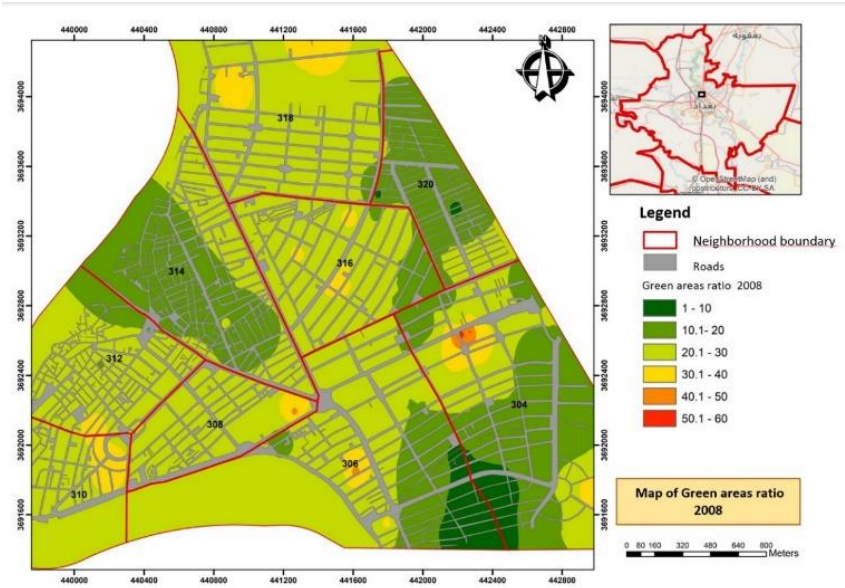

Figure S1. Spatial distribution for urban green areas in Baghdad-Adhamiya 2008

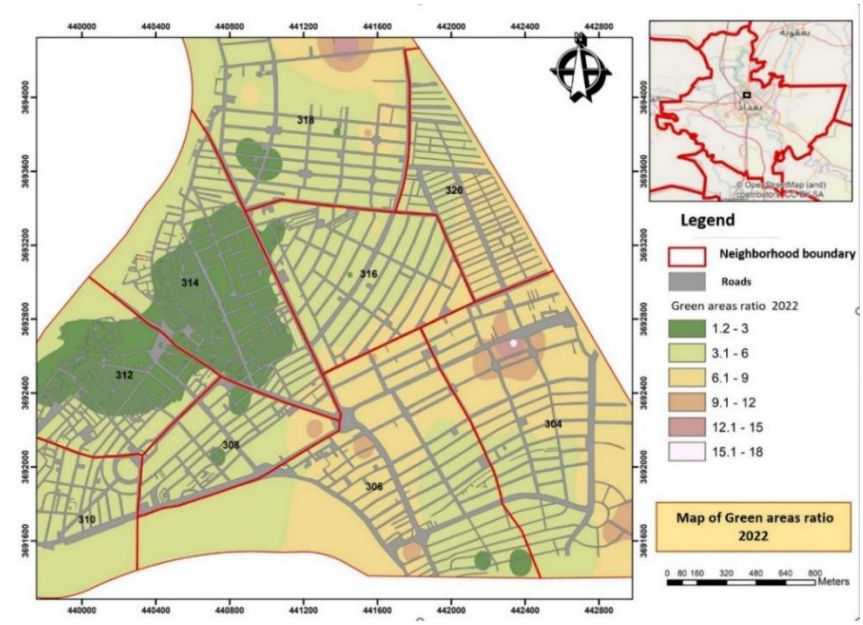

Figure S2. Spatial distribution for urban green areas in Baghdad-Adhamiya 2022